Inorganic Chemistry
Article

Inorg. Chem. **2011**, *50*, 597–603 **597**
DOI: 10.1021/ic1018345

Reversible Solid-State Structural Transformation of a 1D−2D Coordination Polymer by Thermal De/Rehydration Processes

Chih-Chieh Wang,*,† Ching-Chun Yang,† Chang-Tsung Yeh,† Kum-Yi Cheng,† Pei-Chen Chang,† Mei-Lin Ho,*,† Gene-Hsiang Lee,‡ Wei-Ju Shih,§ and Hwo-Shuenn Sheu*,§

†*Department of Chemistry, Soochow University, Taipei, Taiwan,* ‡*Department of Chemistry, National Taiwan University, Taipei, Taiwan, and* §*National Synchrotron Radiation Research Center, Hsinchu, Taiwan*

Received September 7, 2010

A new coordination polymer, $[Zn(HBTC)(BPE)_{0.5}(H_2O)]_n \cdot nH_2O$ (**1**) with an extended 1D ladderlike metal−organic framework (MOF) has been synthesized and structural characterized by single-crystal X-ray diffraction method. Structural determination reveals that, in compound **1**, the Zn(II) ion is four-coordinated in a distorted tetrahedral geometry, bonded to one nitrogen atom from one BPE ligand, and three oxygen atoms from two monodentate carboxylate groups of two $HBTC^{2-}$ ligands and one coordinated water molecule. The $HBTC^{2-}$ acts as a bridging ligand with a bis-monodentate coordination mode, connecting the Zn(II) ions to form a one-dimensional (1D) [Zn(HBTC)] chain. Two 1D chains are then interlinked via the connectivity between the Zn^{II} ions and anti-BPE liagnds to complete the 1D ladderlike MOF. Adjacent 1D Ladders are further extended to a 2D hydrogen-bonded layered network through the intermolecular O−H···O hydrogen bond between the carboxylic group and carboxylate group of interladder $HBTC^{2-}$ ligand. Adjacent 2D layers are then packed orderly in an ABAB-type array via the intermolecular interactions of combined $\pi-\pi$ interaction and O−H···O hydrogen bonds to form a 3D supramolecular architecture exhibiting 1D channels intercalated with guest water molecules. The reversible solid-state structural transformation between crystalline **1** with 1D ladderlike framework and its dehydrated powder **2**, $[Zn(HBTC)(BPE)_{0.5}]_n$, with 2D framework via the displacement of coordinated water molecule to $HBTC^{2-}$ ligand, by thermal de/rehydrated processes has been verified by PXRD measurements. The emission of **1** and **2** is ascribed to a ligand-based transition.

Introduction

Porous coordination polymers or metal−organic frameworks (MOFs) containing guest molecules provide a unique opportunity for developing advanced functional materials and for studying fundamental nanomolecular assemblies in confined spaces.[1] In particular, microporous metal−organic frameworks have received extensive attention because of their potential applications in gas storage[2] and separation, etc.[3] It is now well established that guest molecules may also play a key role by acting as an essential support to the porosity of the host lattice MOFs.[4−6] Crystal-to-crystal transformations involving coordination polymers and networks are more studied recently.[7−22] These kinds of solid-state

*To whom correspondence should be addressed. E-mail: ccwang@scu.edu.tw (C.-C.W.); meilin_ho@scu.edu.tw (M.-L.H.); hsheu@nsrrc.org.tw (H.-S.S.).

(1) (a) Bünzli, J.-C. G.; Piguet, C. *Chem. Soc. Rev.* **2005**, *34*, 1048. (b) Kitagawa, S.; Kitaura, R.; Noro, S.-i. *Angew. Chem., Int. Ed.* **2004**, *43*, 2334 and reference therein.
(2) (a) Rowsell, J. L. C.; Millward, A. R.; Park, K. S.; Yaghi, O. M. *J. Am. Chem. Soc.* **2004**, *126*, 5666. (b) Zhao, X.; Xiao, B.; Fletcher, A. J.; Thomas, K. M.; Bradshaw, D.; Rosseinsky, M. J. *Science* **2004**, *306*, 1012.
(3) (a) Yaghi, O. M.; Davis, C. E.; Li, G.; Li, H. *J. Am. Chem. Soc.* **1997**, *119*, 2861. (b) Maji, T. K.; Uemura, K.; Chang, H.-C.; Matsuda, R.; Kitagawa, S. *Angew. Chem., Int. Ed.* **2004**, *43*, 3269 and references therein.
(4) Chae, H. K.; Siberio-Pérez, D. Y.; Kim, J.; Go, Y.; Eddaoudi, M.; Matzger, A. J.; O'Keeffe, M.; Yaghi, O. M. *Nature* **2004**, *427*, 523.
(5) Sozzani, P.; Bracco, S.; Comotti, A.; Ferretti, L.; Simonutti, R. *Angew. Chem., Int. Ed.* **2005**, *44*, 1816.
(6) Prasad, T. K.; Rajasekharan, M. V. *Cryst. Growth Des.* **2006**, *6*, 488.
(7) (a) Nagarathinam, M.; Vittal, J. J. *Angew. Chem., Int. Ed.* **2006**, *45*, 4337. (b) Toh, N. L.; Nagarathinam, M.; Vittal, J. J. *Angew. Chem., Int. Ed.* **2005**, *44*, 2237. (c) Yang, X. D.; Wu, D.; Ranford, J. D.; Vittal, J. J. *Cryst. Growth Des.* **2005**, *5*, 41.
(8) Kim, T. H.; Shin, Y. W.; Kim, J. S.; Kim, J. *Angew. Chem., Int. Ed.* **2008**, *47*, 685.
(9) Lee, J. Y.; Lee, S. Y.; Sim, W.; Park, K. M.; Kim, J.; Lee, S. S. *J. Am. Chem. Soc.* **2008**, *130*, 6902.
(10) Hu, C.; Englert, U. *Angew. Chem., Int. Ed.* **2005**, *44*, 2281.
(11) Rather, B.; Moulton, B.; Walsh, R. D. B.; Zaworotko, M. J. *Chem. Commun.* **2002**, 694.
(12) Shin, D. M.; Lee, I. S.; Cho, D.; Chung, Y. K. *Inorg. Chem.* **2003**, *42*, 7722.
(13) Xue, X.; Wang, X.-S.; Xiong, R.-G.; You, X. Z.; Abrahams, B. F.; Che, C.-M.; Ju, H.-X. *Angew. Chem., Int. Ed.* **2002**, *41*, 2944.
(14) Oliver, S.; Kuperman, A.; Lough, A.; Ozin, G. A. *Chem. Mater.* **1996**, *8*, 2391.
(15) Lin, W.; Evans, O. R.; Xiong, R. G.; Wang, Z. Y. *J. Am. Chem. Soc.* **1998**, *120*, 13272.
(16) Oh, M.; Carpenter, G. B.; Sweigart, D. A. *Angew. Chem., Int. Ed.* **2001**, *40*, 3191.
(17) Kim, J. H.; Hubig, S. M.; Lindeman, S. V.; Kochi, J. K. *J. Am. Chem. Soc.* **2001**, *123*, 87.
(18) Lotsch, B.; Senker, J.; Schnick, W. *Inorg. Chem.* **2004**, *43*, 895.

Published on Web 12/14/2010

structural transformation not only directly reflect the relationship between the structures involved but also provide the effects on the properties of coordination polymers with small structural changes. Several types of structural transformations are primarily influenced by the following pathways, including the expansions of the metal coordination numbers, thermal dissociation/association, condensation, rearrangement of bonds or the removal or exchange of solvents.[23] In this contribution, we report here the reversible thermal de- and rehydration of a new one-dimensional (1D) ladderlike coordination polymer to a different two-dimensional layered coordination polymer, $[Zn(HBTC)(DPE)_{0.5}(H_2O)]_n \cdot nH_2O$ (**1**) to $[Zn(HBTC)(DPE)_{0.5}]_n$ (**2**), $HBTC^{2-}$ = dianion of trimesic acid, DPE = 1,2-bis-(4-pyridyl)ethane, which is verified by TG measurement, as well as in situ temperature-resolved X-ray powder diffraction identification.

Experimental Section

Materials and Physical Techniques. General: All chemicals were of reagent grade and were used as commercially obtained without further purification. Elemental analyses (carbon, hydrogen, and nitrogen) were performed using a Perkin-Elmer 2400 elemental analyzer. The infrared spectrum was recorded on a Nicolet Fourier Transform IR, MAGNA-IR 500 spectrometer in the range 500−4000 cm^{-1} using the KBr disk technique. Thermogravimetric analysis (TGA) and differential scanning calorimetry (DSC) of the title compound was performed on a computer-controlled Perkin-Elmer 7 Series/UNIX TGA7 analyzer. Single-phased powder sample of **1** (1.371 mg) was loaded into alumina pans and heated with a ramp rate of 5 °C/min from room temperature to 800 °C under nitrogen atmosphere.

Synthesis of $[Zn(HBTC)(DPE)_{0.5}(H_2O)]_n \cdot nH_2O$ (1). Trimesic acid (H_3BTC, 4.2 mg, 0.02 mmol), $ZnCl_2$ (4.1 mg, 0.03 mmol), and 1,2-bis(4-pyridyl)ethane (DPE, 5.5 mg, 0.03 mmol) were dissolved in 9 mL of mixed solvents of distilled water and EtOH (1:1, v/v) at room temperature to give a colorless solution. Colorless blocked crystals were obtained after several days in 12.3% yield. The resulting colorless blocked crystals of **1** were collected by filtration, washed several times with distilled water, and dried in air. Anal. Calcd for $C_{15}H_{13}NO_8Zn$ (M_w = 400.64): C 44.93, N 3.49, H 3.24. Found: C 45.01, N 3.45, H 3.31. IR (KBr pellet): ν = 3401 (w), 3369 (w), 1613 (m), 1556 (vs), 1427 (m), 1225 (s), 769 (m) cm^{-1}.

Crystallographic Data Collection and Refinement. Single-crystal structure analyses of compound **1** was performed on a Siemens SMART diffractomer with a CCD detector with Mo radiation (λ = 0.71073 Å) at room temperature. Cell parameters were retrieved using SMART[24] software and refined with SAINT[25] on all observed reflections. Data reduction was performed with the SAINT[25] software and corrected for Lorentz and polarization effects. Absorption corrections were applied with the program SADABS.[26] Direct phase determination and subsequent difference Fourier map synthesis yielded the positions of all non-hydrogen atoms, which were subjected to anisotropic refinements. All hydrogen atoms were generated geometrically (C−H = 0.93 (C_{sp^2}−H) or 0.97 (C_{sp^3}−H) Å) with the exception of the hydrogen atoms of the coordinated water molecules, which were located in the difference Fourier map with the corresponding positions and isotropic displacement parameters being refined. The final full-matrix, least-squares refinement on F^2 was applied for all observed reflections [$I > 2\sigma(I)$]. All calculations were performed using the SHELXTL-PC V 5.03 software package.[27] Crystallographic data and details of data collections and structure refinements of compound **1** are listed in Table 1.

Table 1. Crystal Data and Refinement Details of $[Zn(HBTC)(dpe)_{0.5}]_n \cdot nH_2O$ (**1**)[a]

chemical formula	$C_{30}H_{28}N_2O_{16}Zn_2$
crystal syst	triclinic
a (Å)	7.0836(3)
b (Å)	9.4336(4)
c (Å)	12.4037(6)
V (Å^3)	769.44(6)
ρ_{calcd}/g cm^{-3}	1.734
μ (mm^{-1})	1.643
total no. of data collected	7850
R_1, R_2 ($I > 2\sigma(I)$)	0.0714, 0.1988
GOF	1.091
formula mass	803.28
space group	$P\bar{1}$
α (deg)	75.948(2)
β (deg)	83.685(2)
γ (deg)	73.303(3)
Z	1
2θ range (deg)	4.62−50.00
T (K)	295(2)
no. of obsd data ($I > 2\sigma(I)$)	2202
R_1, R_2 (all data)	0.0870, 0.2145
no. of variable	227

[a] $R_F = \Sigma\|F_o - F_c\|/\Sigma|F_o|$; $R_2(F^2) = [\Sigma w|F_o^2 - F_c^2|^2/\Sigma w(F_o^4)]^{1/2}$.

CCDC-792151 for **1** contains the supplementary crystallographic data for this paper. These data can be obtained free of charge at www.ccdc.cam.ac.uk/conts/retrieving.html [or from the Cambridge Crystallographic Data Centre, 12, Union Road, Cambridge CB2 1EZ, U.K.; fax: (Internet.) +44−1223/336−033; E-mail: deposit@ccdc.cam.ac.uk].

In Situ X-ray Powder Diffraction of 1. The powder X-ray diffraction patterns of **1** were recorded at the BL01C2 beamline of the National Synchrotron Radiation Research Center (NSRRC) in Taiwan. The ring energy of NSRRC was operated at 1.5 GeV with a typical current of 300 mA. The wavelength of the incident X-rays was 1.0332 Å (12.0 keV), delivered from the superconducting wavelength-shifting magnet, and a Si(111) double-crystal monochromator. The diffraction patterns were recorded with a Mar345 imaging plate detector approximately 300 mm from sample positions and typical exposure duration 5 min. The pixel size of Mar345 was 100 μm. The one-dimensional powder diffraction profile was converted with program FIT2D and cake-type integration. The diffraction angles were calibrated according to Bragg positions of Ag-Benhenate and Si powder (NBS640b) standards. In situ synchrotron X-ray powder diffraction for **1** was performed at BL01C2 from 28 to 450 °C with a heating rate approximately 10 °C/min. The powder sample was sealed in a capillary (1.0 mm diameter) and heated in a stream of hot air; each in situ powder XRD pattern was exposed for about 1.2 min.

(19) (a) Mahmoudi, G.; Morsali, A. *Cryst. Growth Des.* **2008**, *8*, 391. (b) Aslani, A.; Morsali, A.; Zeller, M. *Dalton. Trans.* **2008**, 5173. (c) Aslani, A.; Morsali, A. *Chem. Commun.* **2008**, 3402.
(20) (a) Habib, H. A.; Sanchiz, J.; Janiak, C. *Dalton. Trans.* **2008**, 1734. (b) Ye, J.; Liu, Y.; Zhao, Y.; Mu, X.; Zhang, P.; Wang, Y. *CrystEngComm* **2008**, *10*, 598.
(21) (a) Sadeghzadeh, H.; Morsali, A. *Inorg. Chem.* **2009**, *48*, 10871. (b) Khanpour, M.; Morsali, A. *CrystEngComm* **2009**, *11*, 2585. (c) Khanjani, S.; Morsali, A.; Retailleau, P. *CrystEngComm* **2010**, *12*, 2173. (d) Khanpour, M.; Morsali, A. *Eur. J. Inorg. Chem.* **2010**, 1567.
(22) (a) Ranford, J. D.; Vittal, J. J.; Wu, D. *Angew. Chem., Int. Ed.* **1998**, *37*, 1114. (b) Vittal, J. J. In *Frontiers in Crystal Engineering*; Tiekink, E. R. T.; Vittal, J. J., Eds.; John Wiley & Sons: Chichester, U.K., 2006; Chapter12, p 297.
(23) Vittal, J. J. *Coord. Chem. Rev.* **2007**, *251*, 17.
(24) *SMART V 4.043 Software for CCD Detector System*; Siemens Analytical Instruments Division: Madison, WI, 1995.
(25) *SAINT V 4.035 Software for CCD Detector System*; Siemens Analytical Instruments Division: Madison, WI, 1995.
(26) Sheldrick, G. M. *Program for the Refinement of Crystal Structures*; University of Göttingen: Göttingen, Germany, 1993.
(27) *SHELXTL 5.03* (*PC-Version*), *Program Liberary for Structure Solution and Molecular Graphics*; Siemens Analytical Instruments Division: Madison, WI, 1995.

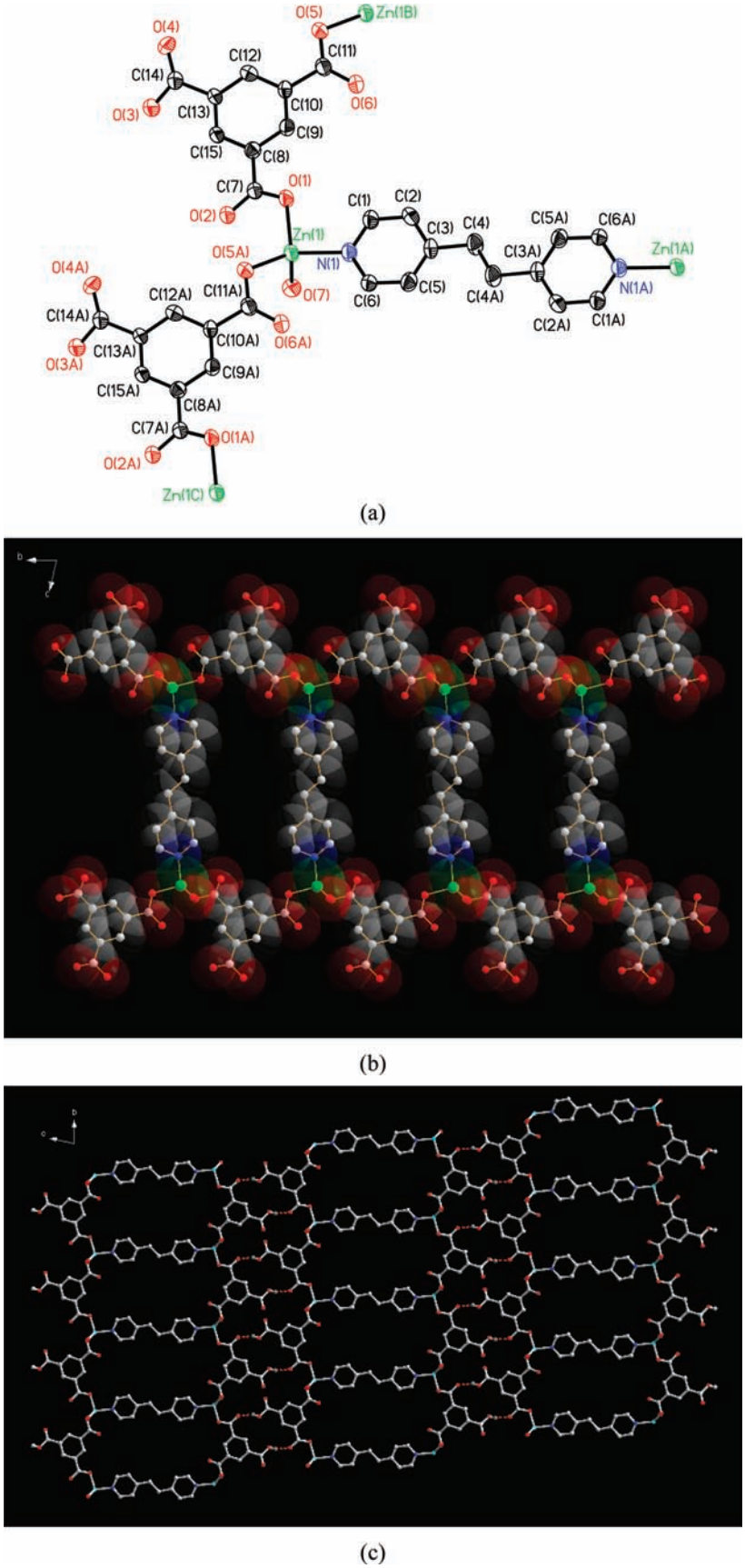

Figure 1. (a) Coordination sphere about Zn^{II} of **1** with atom labeling scheme. Selected bond length (Å) and angles (deg): Zn(1)−O(1) 1.962(4), Zn(1)−N(1) 2.009(5), Zn(1)−O(7) 2.022(5), Zn(1)−O(5A) 1.937(4), O(5A)−Zn(1)−O(1) 112.9(2), O(5A)−Zn(1)−N(1) 130.3(2), O(5A)−Zn(1)−O(7) 104.5(2), O(1)−Zn(1)−N(1) 99.1(2), O(1)−Zn(1)−O(7) 105.9(2), N(1)−Zn(1)−O(7) 101.8(2). (A = $x, y + 1, z$) Lattice water molecule is omitted for clarity (ORTEP drawing, 50% thermal ellipsoids). (b) The 1D ladderlike framework was formed by the Zn(II) ions, DPE and $HBTC^{2-}$ ligands. (c) The 2D hydrogen-bonded layered network via the O(3)−H(3)···O(2) hydrogen bonds between $HBTC^{2-}$ ligands among the 1D ladderlike MOFs.

The dehydrated structure for $[Zn(HBTC)(DPE)_{0.5}]_n$ **2** at 180 °C was determined from the powder diffraction data with program DASH. Powder pattern was indexed with Dicvol and Treor programs. The structure factors of the powder patterns were extracted with Pawley's method, and simulated annealing was employed to determine the crystal structure. The final refinement with the Rietveld method was performed using GSAS program.

Spectral Measurement. UV−vis diffuse reflectance spectra of crystal **1** and **2** were obtained with a HITACHI U-3900H spectrophotometer equipped with an integrating sphere accessory (Al_2O_3 was used as a reference). To investigate the differences in photoluminescence of **1** and **2** due to the variation of topologies, **1** and **2** were measured with a confocal mode of a MonoVista confocal Raman microscope system (Princeton Instruments/Acton) using a Linkam THMS 600 hot stage (Linkam Scientific Instruments, United Kingdom) equipped with a video camera (QImage 5.0 RTV), in which the optics have been specially made to allow both UV (up to 280 nm) excitation and emission. Microscope (Olympus BX51) is with an upright-style frame in which all optics are modified to allow the passage of deep UV to infrared light. The photoluminescence spectra of **1** and **2** were acquired using a Linkam temperature controller (T95-LinkPad; Linkam Scientific Instruments, United Kingdom) for hot stage control. In this approach, a 325 nm laser line (He−Cd laser, KIMMON IK3301R-G) was used as an excitation source throughout the measurement. A set of neutral density filters is then placed in the beam path to attenuate the laser power. The photoluminescence was separated from the scattering light of excitation pulse by a edge filter with a cutoff wavelength of 325 nm (333AELP, Omega Optical) and sent by an optical fiber to the entrance slit of a polychromator (blazed at 500 nm) coupled with a sensitive charge coupled detector (CCD, Princeton Instruments, PI-MAX). The CCD was operated in a shutter mode and the measurements were performed with 100 ms exposure time. All spectra were accumulated over an average 1 scan.

Results and Discussion

Structure Description of $[Zn(HBTC)(DPE)_{0.5}(H_2O)]_n \cdot nH_2O$ (1). Compound **1**, $[Zn(HBTC)(DPE)_{0.5}(H_2O)]_n \cdot nH_2O$, was synthesized by using $ZnCl_2$, trimesic acid (H_3BTC) and 1,2-bis-(4-pyridyl)ethane (DPE) in the mixed solvents of distilled water and EtOH (1:1, v/v) at room temperature. The molecular structure of the fundamental building unit for **1** is shown in Figure 1a. In **1**, the Zn^{II} ion is four-coordinated in a distorted tetrahedral geometry bonded with one nitrogen atom (N1) from DPE ligand, two oxygen atoms (O1 and O5A; symmetry transformation A = $+x$, $1+y$, $+z$) from two $HBTC^{2-}$ ligands and one water molecule (O7). The corresponding bond lengths and angles around the Zn^{II} center are listed in Table 2. The $HBTC^{2-}$ ligand acts as a bridging ligand with bis-monodentate coordination mode connecting the Zn^{II} centers to form a 1D linear chain. Two chains are connected together via the linkage of the Zn^{II} ions and bis-monodentate anti-DPE ligand, forming a 1D ladderlike metal−organic framework (MOF) as shown in Figure 1b. The Zn···Zn separations bridged by the $HBTC^{2-}$ and DPE ligands are 9.434(2) Å and 13.429(5) Å, respectively.

The most remarkable and interesting features on the construction of its 3D supramolecular architectures in **1** is that the subtle combination of hydrogen bonding and $\pi\cdots\pi$ stacking interactions serves to connect these 1D ladderlike coordination chains to 2D layered networks, and then a 3D supramolecular architecture, as shown in Figure 1c, and Figure S1 (see in the Supporting Information), respectively. First, these adjacent 1D ladderlike MOFs are mutually interlinked via the strong interladder O(3)−H(3)···O(2) hydrogen bonds between the carboxylic and carboxylate groups of $HBTC^{2-}$ ligands with O···O distance of 2.540(7) Å (Table 3) and extended to a 2D hydrogen-bonded layered network (Figure 1c). These 2D hydrogen-bonded layers are arrayed orderly in an staggered ABAB... packing pattern and then extended to a 3D network, via the $\pi-\pi$ interactions between the benzene ring of $HBTC^{2-}$ and pyridyl ring of DPE (related interplanar parameters see Table 4) and intermolecular O−H···O hydrogen bonds between the coordinated water molecules (O(7)) and uncoordinated oxygen atom (O(6)) of carboxylate groups of $HBTC^{2-}$ ligand with O···O distance of 2.686(8) Å. The solvated water molecules are intercalated into the micropores formed in the 3D network. The 3D supramolecular architecture is further reinforced by the O−H···O hydrogen bonding among the solvated water molecules, coordinated water molecules, and $HBTC^{2-}$ ligands (see Table 3 and Figure S1 in the Supporting Information).

Table 2. Bond Lengths (Å) and Angles (deg) around Zn(1) ion in **1**[a]

$Zn(1)-O(5)_i$	1.937(4)	Zn(1)−O(1)	1.962(4)
Zn(1)−N(1)	2.009(5)	Zn(1)−O(7)	2.022(5)
$O(5)_i-Zn(1)-O(1)$	112.9(2)	$O(5)_i-Zn(1)-N(1)$	130.3(2)
O(1)−Zn(1)−N(1)	99.1(2)	$O(5)_i-Zn(1)-O(7)$	104.5(2)
O(1)−Zn(1)−O(7)	105.9(2)	N(1)−Zn(1)−O(7)	101.8(2)

[a] Symmetry transformations used to generate equivalent atoms: i = $x, y+1, z$.

Table 3. O−H···O Hydrogen Bonds for **1**[a]

D−H···A (Å)	D−H (Å)	H···A (Å)	D···A (Å)	∠D−H···A (deg)
$O(3)-H(3)\cdots O(2)_i$	0.820(5)	1.75	2.540(7)	160.0
$O(7)-H(7A)\cdots O(8)_{ii}$	0.896(5)	1.84	2.734(8)	175.6
$O(7)-H(7B)\cdots O(6)_{iii}$	0.897(5)	1.80	2.686(8)	174.1
$O(8)-H(8A)\cdots O(4)_{iv}$	0.899(6)	2.32	2.976(8)	130.3
$O(8)-H(8B)\cdots O(4)_v$	0.903(7)	2.32	2.900(9)	122.1

[a] Symmetry codes used to generate equivalent atoms: i = $2-x, -1-y, -1-z$; ii = $1-x, -y, -z$; iii = $1-x, -1-y, -z$; iv = $-1+x, 1+y, 1+z$; v = $2-x, -1-y, -z$.

Thermogravimetric Analysis, Thermal Stability and Reversible Solvent De/Adsorption. To assess the thermal stability and its structural variation as a function of the temperature, thermal gravimetric and differential scanning calorimetry analyses (TGA and DSC) were recorded for the single-phase polycrystalline samples. During the heating process, TGA (shown in Figure S2a in the Supporting Information) revealed that compound **1** underwent a two-step weight loss and thermally stable up to 100 °C with the weight loss of 9.7% (calcd 9.0%) and an endothermic effect around 105 °C (shown in Figure S2b in the Supporting Information), corresponding to the loss of coordinated and solvated water molecules. The dehydrated framework is stable up to 290 °C and decomposition takes places between 290−447 °C with a mass loss ~69.9%. The solid residue formed at around 447 °C is suggested to be ZnO (found 20.2%, calc 20.3%). To verify the ab/desorption of solvated and coordinated water molecules in **1**, we have studied the de- and rehydration processes

Table 4. $\pi-\pi$ Interactions (Face-to-Face) in **1**[a]

ring(i) → ring(j)	slip angle[b] (i,j)/deg	interplanar (i,j) distance[c]/Å	horizontal shift between the (i,j) ring centroids[d]/Å	distance between the (i,j) ring centroids/Å
R(1) → R(2)$_{i}$	28.6	3.403	1.858	3.877
R(2) → R(1)$_{ii}$	28.7	3.402	1.860	3.877
R(1) → R(2)$_{ii}$	37.8	3.318	2.577	4.201
R(2) → R(1)$_{i}$	36.2	3.388	2.484	4.201

[a] Symmetry code: I = $-x+1, -y-1, -z$; ii = $-x+2, -y-1, -z$. R(i)/R(j) denotes the centroids of ith/jth of croconate/croconate; R(1) = C(8)−C(9)−C(10)−C(12)−C(13)−C(15), R(2) = N(1)−C(1)−C(2)−C(3)−C(5)−C(6). [b] Slip angle: The angle formed between the ring-centroid vector (CC) and the ring normal to one of the croconate planes. [c] Interplanar distance: The perpendicular distance between two parallel rings. [d] Horizontal shift between the ring centroids: a shift from the face-to-face alignment.

of **1** by TG measurements under water vapor. Interestingly, the water molecules can be adsorbed fully by exposing the samples to water vapor when the sample was cooled to room temperature. The heating and cooling procedures were repeated for three times to demonstrate the reversibility of the de- and rehydration processes (see Figure S2c in the Supporting Information). Similar de- and adsorption phenomenon can also be observed, instead of water to methanol and ethanol solvents (see Figure S2d and e in the Supporting Information).

In Situ PXRD Studies of 1 and Dehydrated [Zn(HBTC)(DPE)$_{0.5}$]$_n$ (2). High-resolution powder diffraction patterns of **1** were studied using synchrotron radiation. Single crystal structure of **1** was used as initial model for Rietveld method refinement for the powder crystalline structure at room temperature (see Figure S3 in the Supporting Information). The thermostability of **1**, as well as its phase transitions, was also investigated by in situ powder diffraction as shown in Figure 2. The powder crystalline structure at room temperature is matching well to its single crystal structure. The powder pattern of **1** at room temperature was similar to that of 120 °C but begun to change at 150 °C. A new crystalline phase was found during 180−330 °C. The crystal structure of **1** at 120 °C can be refined by using the model at room temperature, only that the occupancy of solvated water molecules (O8) becomes less. This result indicates that the solvated water molecule begun to lose at 120 °C. The powder pattern at 150 °C cannot be indexed as a simple unit cell, which indicated that the crystalline structure at 150 °C may be either a super large unit cell or a multiphase. Therefore, we try to index the powder pattern at 180 °C and, fortunately, the powder pattern can be indexed by Dicvol program that yield a new unit cell with $P\bar{1}$ space group (Table 5). It is noticeable that the molecular structure obtained by PXRD at 180 °C is a dehydrated form of [Zn(HBTC)(DPE)$_{0.5}$]$_n$ **2** as shown in Figure 3. The oxygen atom (O(6)) of organic $HBTC^{2-}$ ligand shifts toward the Zn(II) ion and replaces the water molecule (O(7)) to coordinate to Zn(II) ion, which play an key role on the linkage of adjacent 1D ladderlike frameworks to 2D framework as shown in Figure 3(b). Importantly, the strong hydrogen bond found between O(2) and O(3) in **1** is also existed in the dehydrated **2** at 180 °C with the O···O distance of 2.583 Å which connected these 2D frameworks became a 3D hydrogen-bonded supramolecular network. After we solved the crystalline structure of dehydrated **2** at 180 °C, the structure of the PXRD pattern at 150 °C can thus be refined by the combination of two phases crystalline with 42.1% of **1** and 57.9% of **2**, respectively (see Figure S3b in the Supporting Information). Rietveld refinement results of in situ powder patterns were listed in Table 5. The PXRD measurements are in accordance with the TGA/DTA and both results evidence that **1** undergo a structural transformation to dehydrated **2** driven by dehydration process, which is thermal stable up to 300 °C.

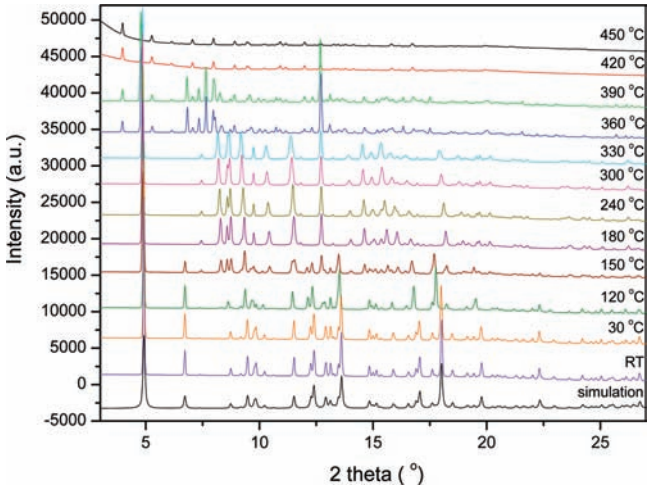

Figure 2. In situ temperature-dependent powder XRD of **1**.

Solid-State Structural Transformation by Thermal De/Rehydration Processes. The most promising feature of the crystals of **1** is that they undergo a reversible solid-state structural transformation driven by thermal dehydration and rehydration. However, when a dehydrated sample of **2** at 200 °C (Figure 4b) is cooled down to RT and exposed to water (i.e., the dehydrated sample is placed in a glass capillary, beside a beaker filled with water) it reabsorbs the lost coordinated and solvated water molecules. The PXRD pattern of the rehydrated species (Figure 4c) shows that the sample regains the original structure **1** and is re-established as the rehydrated species showing almost the same PXRD diffractogram as that of as the freshly synthesized material (Figure 4d). The coordination geometry of the Zn(II) ions in the 1D coordination polymer [Zn(HBTC)(DPE)$_{0.5}$(H_2O)]$_n$·$n$$H_2O$ (**1**) and 2D [Zn(HBTC)(DPE)$_{0.5}$]$_n$ (**2**) induces some inspiration about the origin and mechanism of the solid-state transformation.[28] A schematic representation of this structural transfer is shown in Figure 5. The coordinated water molecules in **1** are stacked roughly on the top and down of each layer and

(28) Attempts to measure the unit cell of the dehydrated **2** by single crystal diffraction method were not successful because the crystal split into several pieces when mounted on the single-crystal diffractometer even upon heating compound **1** slowly.

Table 5. Crystal Data of **1** and **2** Obtained from Single-Crystal XRD and In Situ Powder XRD at 30, 120, 150, 180, and 300 °C

parameters	single crystal	powder	powder	powder		powder	powder
temperature (°C)	22	30	120	150		180	300
formula	$C_{15}H_{13}N_1O_8Zn_1$	$C_{15}H_{13}N_1O_8Zn_1$	$C_{15}H_{13}N_1O_8Zn_1$	$C_{15}H_{11}N_1O_7Zn_1$	$C_{15}H_9N_1O_6Zn_1$	$C_{15}H_9N_1O_6Zn_1$	$C_{15}H_9N_1O_6Zn_1$
phase (wt. frac%)	I (100)	I (100)	I (100)	I (42.09)	II (57.91)	II(100)	II (100)
space group	$P\bar{1}$	$P\bar{1}$	$P\bar{1}$	$P\bar{1}$	$P\bar{1}$	$P\bar{1}$	$P\bar{1}$
Z	2	2	2	2	2	2	2
wavelength, (Å)	0.71073	1.0332	1.0332	1.0332	1.0332	1.0332	1.0332
a, (Å)	7.0836(3)	7.0939(2)	7.1889(3)	7.2205(9)	7.6815(8)	7.7033(4)	7.8030(4)
b, (Å)	9.4336(4)	9.4410(3)	9.4483(4)	9.437(1)	8.425(1)	8.4296(7)	8.4422(7)
c, (Å)	12.4037(6)	12.4163(4)	12.4369(5)	12.412(2)	12.516(2)	12.5436(7)	12.5526(7)
α, (deg)	75.948(2)	75.868(5)	75.778(6)	75.72(2)	98.39(2)	98.438(8)	98.467(8)
β, (deg)	83.685(2)	83.614(4)	83.187(5)	83.02(2)	103.52(1)	103.542(7)	103.355(7)
γ, (deg)	73.303(3)	73.218(4)	73.937(3)	72.74(1)	71.21(1)	71.120(6)	70.607(6)
V	769.44(6)	771.37(3)	781.83(4)	781.7(1)	743.4(1)	747.05(6)	756.65(7)
R_1	0.0719						
R_2	0.2002						
wR_p		0.0280	0.0297	0.0375		0.0272	0.0336
R_p		0.0173	0.0193	0.0241		0.0157	0.0206
χ^2		0.622	0.777	1.858		1.014	1.121

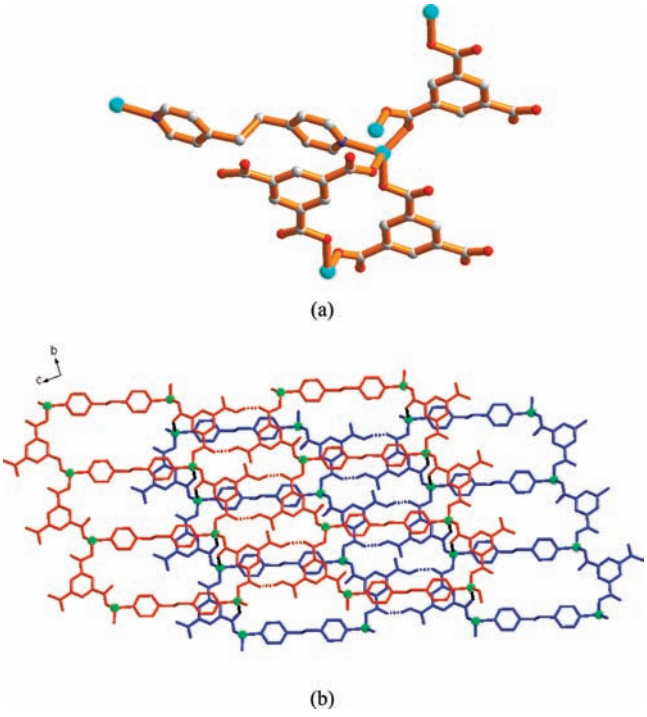

Figure 3. (a) Molecular structure of dehydrated **2** at 180 °C. (b) 2D framework of **2** via the bridges of Zn(II) ion with O(6) atom of $HBTC^{2-}$ ligands.

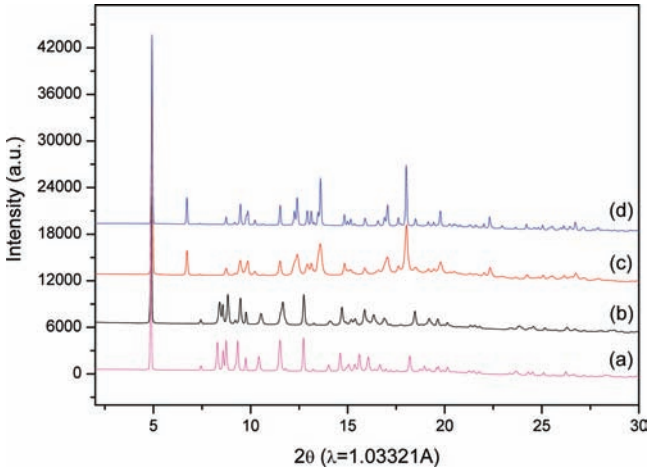

Figure 4. PXRD patterns of (a) dehydrated samples **2** at 180 °C and (b) dehydrated samples at 200 °C sealed in vacuum. (c) Rehydrated samples obtained by exposure of the dehydrated samples (b) to water vapor for 1 week. (d) The fresh samples as synthesized for **1**.

the removal of the water molecules would create open channels through the entire crystal, which would allow for relatively easy and nondestructive removal of all the solvated molecules. Meanwhile, the uncoordinated oxygen atoms (O(6)) of carboxylate groups of $HBTC^{2-}$ dianions in **1** are also oriented toward to the coordinated water molecules (O(7)) of neighboring units via O(7)−H(7B)···O(6) hydrogen bonds (Figure 5 top dashed line in red color and Table 3). It can be assume that, upon the removal of coordinated water molecules by thermal process, these intermolecular contracts shorten in the course of the solid-state reaction and turn into bonds with Zn(II) ions (Figure 5 bottom dashed line in black color) by removal of the water molecules, creating a new 2D network topology of (**2**).

Luminescence Properties of 1 and 2. Taking the latent luminescence of d^{10} metal complexes into account, the luminescence properties of both free ligands (H_3BTC and DPE) and **1** and **2** were then investigated. Figure S5a (Supporting Information) reveals the solid state absorption and single crystal emission for **1** and **2**. All luminescence are acquired with a confocal microscope equipped with a He−Cd laser as the excitation source (see Experimental Section for detail). Upon excitation at, for example, 325 nm, as depicted in Figure S5b (Supporting Information), compound **1** exhibits a moderate, blue emission band maximized at ~410 nm. The lifetime of ~1.8 ns ensures its origin from a singlet manifold, that is, the fluorescence. Moreover, the same emission spectral features were resolved throughout different probing areas of the crystals, ruling out the possibility that the emission originates from any crystal defects. Prior to the discussion, we have also performed a control experiment to acquire the spectrum of single crystal H_3BTC and DPE under identical experimental condition (see Figure S5a in the Supporting Information). The photoluminescence of ligand H_3BTC and DPE single crystal both exhibits weak fluorescence maximized at ~410 and ~470 nm, respectively. The emission have been assigned to the $\pi^* \rightarrow$ n and DPE excimer-like emission, respectively.[29] Upon coordination

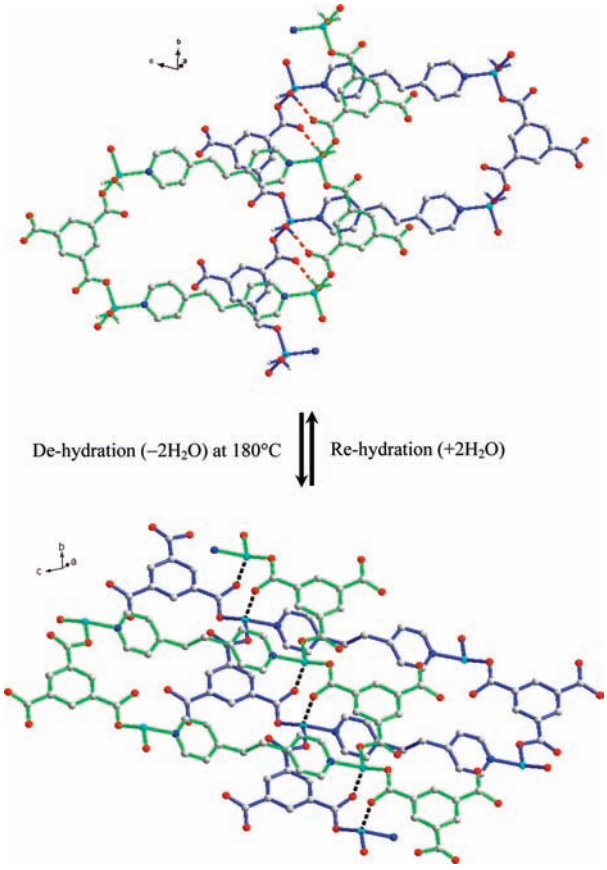

Figure 5. Schematic diagram illustrates the structural conversion of 1D to 2D coordination polymeric structures by thermal de- and rehydration.

with zinc metal cations, the 325 nm excitation, a hypsochromic shift accompanied by an increased emission intensity of compound **1** was observed. In comparison with the position and intensity of emission bands of free ligands, the fluorescence of **1**, seems not to originate from the associated $\pi^* \rightarrow$ n and DPE excimer-like emission, but arises from the charge-transfer transition.[29a,30]

Interestingly, upon increasing temperatures from RT to ~180 °C (see Figure S5b in the Supporting Information), corresponding to the formation of compound **2**, the fluorescence peak wavelength hypsochromically shifts to 350 nm (~180 °C). Such changes are also accompanied by a 2-fold increase of the emission intensity. Also, the lifetime for compound **2** was measured to be 2.3 ns, which is similar to compound **1**. Accordingly, the emissions of compounds **1** and **2** are mainly ascribed to ligand-based transitions. Note that such reversible photoluminescence behavior can be clearly viewed by naked eyes, as shown in inset of Figure S5b (Supporting Information).

Conclusions

In summary, the 1D ladderlike MOF, $[Zn(HBTC)(DPE)_{0.5}(H_2O)]_n \cdot nH_2O$ (**1**), dehydrates up heating of the solid to 180 °C to form a new 2D MOF, $[Zn(HBTC)(DPE)_{0.5}]_n$ (**2**). In the crystal lattice, one oxygen atom of the uncoordinated carboxylate group of $HBTC^{2-}$ ligand moves toward the neighboring Zn(II) ion, with concomitant removal of the water molecule, and form a new Zn−O bond without expanding the coordination geometry of metal center. The reversibility of the solid transformation has been supported by the TGA, PXRD, photoluminescence studies and show that the process is reversible and nondestructive and **1** can be regenerated form **2** upon exposure to water vapor.

Acknowledgment. The authors wish to thank the National Science Council (NSC), Taiwan ROC for financial support.

Supporting Information Available: Figures showing thermogravimetric measurement, cyclic de/adsorption processes, powder X-ray diffraction patterns, and photoluminescence spectra. This material is available free of charge via the Internet at http://pubs.acs.org.

(29) (a) Chen, W.; Wang, J.-Y.; Chen, C.; Yue, Q.; Yuan, H.-M.; Chen, J.-S.; Wang, S.-N. *Inorg. Chem.* **2003**, *42*, 944. (b) Mahmoudi, G.; Morsali, A.; Zhu, L.-G. *Polyhedron* **2007**, *26*, 2885. (c) Handa, T.; Utena, Y.; Yajima, H. *J. Phys. Chem.* **1984**, *88*, 5150.

(30) Fang, Q.; Zhu, G.; Xue, M.; Sun, J.; Sun, F.; Qiu, S. *Inorg. Chem.* **2006**, *45*, 3582.